HOMOGENIZATION OF METRIC HAMILTON-JACOBI EQUATIONS

ADAM M. OBERMAN, RYO TAKEI, AND ALEX VLADIMIRSKY

ABSTRACT. The objective of this work is the effective numerical solution of front propagation problems in multiscale media. We present a new approach which relates the cell problem for Hamitlon-Jacobi equation, the variational formulation for the Lagrangian, and the variational formulation for the metric. The main advantage of our approach is that we solve *just one auxiliary equation* to recover the homogenized Hamiltonian $\bar{H}(p)$. Previous methods require the solution of the cell problem (or a variational problem for each value of p. Computational results are presented in the periodic case for the checkerboard pattern, and several other patterns. Exact solutions are recovered numerically. We also present calculations in the random case.

CONTENTS

1. Introduction

sec:intro

The objective of this work is the effective numerical method for front propagation problems in multiscale media. The wide separation of spatial scales prohibits the direct solution of the fully resolved problem. Instead, the medium which varies on small scales is replaced by a homogeneous medium, which approximates the propagation of the fronts on the larger scale.

We do not derive new analytic homogenization formulas in this work. Instead, we relate several different methods for homogenization, the cell problem for Hamitlon-Jacobi equation, the variational formulation for the Lagrangian, and the variational formulation for the metric, to arrive at a new, simpler and more efficient method for homogenizing front propagation in small scale media. The main idea is to recognize that the distance function in the homogenized metric captures the solution to a variational problem for the geodesics in multiple directions. Thus, this distance function, which can be approximated by solving one Hamilton-Jacobi equation, can be used to recover the entire homogenized metric. To make this procedure work, we need to be able to easily translate results for anisotropic front propagation between various formulations (reviewed in section §2).

The first formulation expresses the speed of propagation in the media by a local speed function. The speed function induces a metric on the space, given by the least time to traverse using admissible paths, see Figure 2. The distance function in this metric satisfies an eikonal-type Hamilton-Jacobi equation, which is also the equation which expresses the normal velocity of fronts. Our results also apply to the time-dependent case, where the homogenized Hamiltonian is the same, and to the homogeneous order two case $H(p,x)^2$, where the homogenized Hamiltonian is $\bar{H}(p)^2$.

Another natural definition of metric in an inhomogeneous medium is provided by the *geodesic distance*. In this case, the velocity along admissible paths is not restricted, but instead a cost function is minimized. The same metric is obtained when that cost function is related to the speed function by a formula explained in §2.7. The advantage of the geodesic formulation is that it leads to a more tractable homogenization problem: the homogenization of Finsler metrics [2].

The main advantage of our approach is that we solve *just one auxiliary equation to recover the homogenized Lagrangian $\bar{L}(q)$ for all values of q.* A Legendre transform can be then applied to obtain $\bar{H}(p)$ for all values of p. For the other currently used methods approximating $\bar{H}(p)$, *a non-linear eigenvalue problem must be solved for each value of p.* The main theoretical result of the paper is derived in section §3, the algorithmic details of our numerical method are provided in section §4, and the numerical results can be found in section §5. But first, we provide the basic background on front propagation and homogenization and describe several model problems in section §1.

1.1. **Particle speeds and front normal velocities.**
Suppose Γ is the initial position of the front and the front is advancing monotonically, passing through each point only once. Furthermore, we will assume that the front's normal speed $F(x, n)$ locally depends on its current position and orientation (i.e., its normal direction n) only. If $u(x)$ is the time when the front passes through the point x, then the level-sets of u give subsequent positions of the front. If the front remains smooth, its normal direction is $n = \frac{\nabla u}{|\nabla u|}$ and the rate of increase of u in that direction is equal $|\nabla u|$. On the other hand, this rate of increase should be the reciprocal of the front's normal speed F. This yields the following static Hamilton-Jacobi equation

$$F\left(x, \frac{\nabla u}{|\nabla u|}\right)|\nabla u| = 1$$

with the boundary condition $u = 0$ on Γ. Since the advancing front will generally not remain smooth, the notion of *viscosity solutions* should be used to interpret this PDE [12].

A Lagrangian (or variational) formulation of the same problem results from considering a front as an aggregate of infinitely many particles, all of which are moving along "optimal" trajectories, with the goal of advancing in the front's normal direction as quickly as possible. The optimal particle-trajectories coincide with the characteristics of the above PDE, and the front remains smooth as long as these optimal trajectories do not intersect.

In order to properly link the Hamilton-Jacobi equation with the Lagrangian formulation, we need to be particularly careful when dealing with anisotropic speeds. In the isotropic case, $F(x, n) = F(x)$ and the optimal direction for particle-travel is also orthogonal to the front, yielding
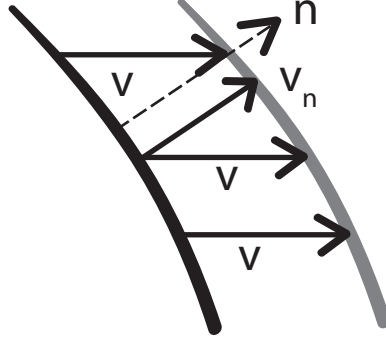
Figure 1: Illustration of normal front speed versus particle speed.   `fig:front`

$F(x) = c(x)$ and the Eikonal PDE

$$c(x)|\nabla u| = 1.$$

In the anisotropic case, the normal velocity of the front is different from the velocity of the moving particles which make up that front.

Example. Suppose particles move horizontally with speed 1, and have no vertical speed allowed. Then the front with normal $(1,1)/\sqrt{2}$ moves with speed $1/\sqrt{2}$ in the normal direction, whereas a vertical front moves at speed 1 and a horizontal front does not move at all. See Figure 1.

The example above can be extended to the general case, where the allowable particle speed in the direction α is given by $c(x, \alpha)$. All particles try to advance the front as quickly as possible; so the optimal direction for particle-motion will depend on the local orientation of the front. In that case, the normal speed of the front is

$$F(x, n) = \max_{\|\alpha\| \leq 1} \{(n \cdot \alpha)c(x, \alpha)\},$$

and the maximizing α corresponds to the direction of particle motion. This connection is discussed in detail in section §2.4. Here we simply note that the front-crossing-time function $T(x)$ is the viscosity solution of the Hamilton-Jacobi equation $H(\nabla T(x), x) = 1$, where the Hamiltonian is given by

`HfromSpeed`   (1) $$H(p, x) := \max_{\|\alpha\| = 1} \{(p \cdot \alpha)c(x, \alpha)\} = |p|F\left(x, \frac{p}{|p|}\right).$$

Before going into the details of our approach, we present a model problem. We first introduce a sample homogenization problem, and then the three scale problem, which combines several homogenization problems.
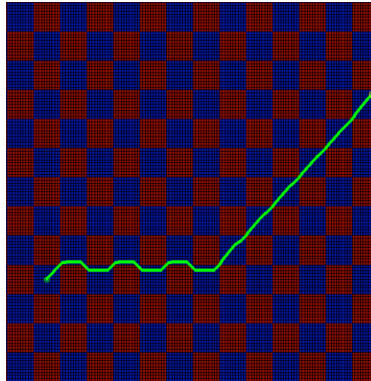
Figure 2: An optimal path in the $(2, 1)$ direction for the checkerboard material. `fig:path`

1.2. Model problem: the periodic checkerboard.

Consider a periodic checkerboard, where the speed is either 1 or 2. Suppose further the front propagation problem is on a scale much larger that the width of each square, and the limited computational resources available are not sufficient to resolve the small scale. Clearly, simply solving on a coarse grid could produce incorrect results, because it could completely miss one of the two materials. This is where *homogenization* comes in: we need to replace the block which varies on small scales with an approximation which captures the large scale behavior of the material with respect to front propagation.

The homogenized material can be found by finding the explicit optimal paths (which are not unique). In this case, if the ratio of speeds is large enough, there is no point spending any time in the slower material. For horizontal, vertical and diagonal directions, up to small oscillations on the scale of ϵ, the paths stay in the fast squares, and move directly. But for the path of slope 2, there is no straight line path, so the optimal path is longer than in the Euclidean case. As a result, the homogenized speed is slower for these directions. See Figure 2. The checkerboard homogenizes to a material whose vectogram is octagonal. We represent the speed of propagation by a *vectogram* which illustrates the speed in each possible direction permitted by the material. See Figure 3. This example illustrates a general principle, *anisotropy can develop as a result of homogenization.*

1.3. Model problem: the random checkerboard.

The random case, where each square is fast or slow with probability one half, is shown in Figure 4. In this case, numerical results suggest that homogenized material is isotropic with speed faster than the harmonic mean, see Figure 14 and the discussion below.

`toy3scale`
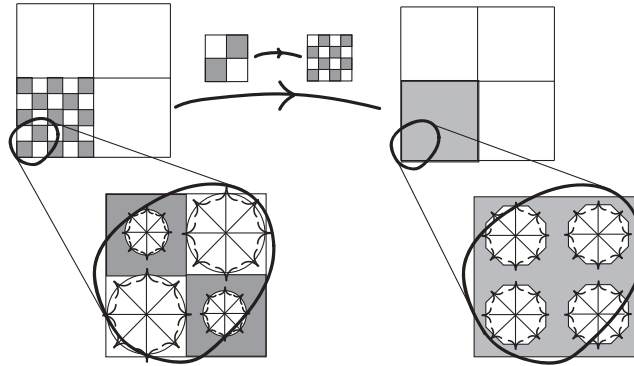
Figure 3: Homogenization of the checkerboard material, illustrated with `fig:checkerboard` vectograms.
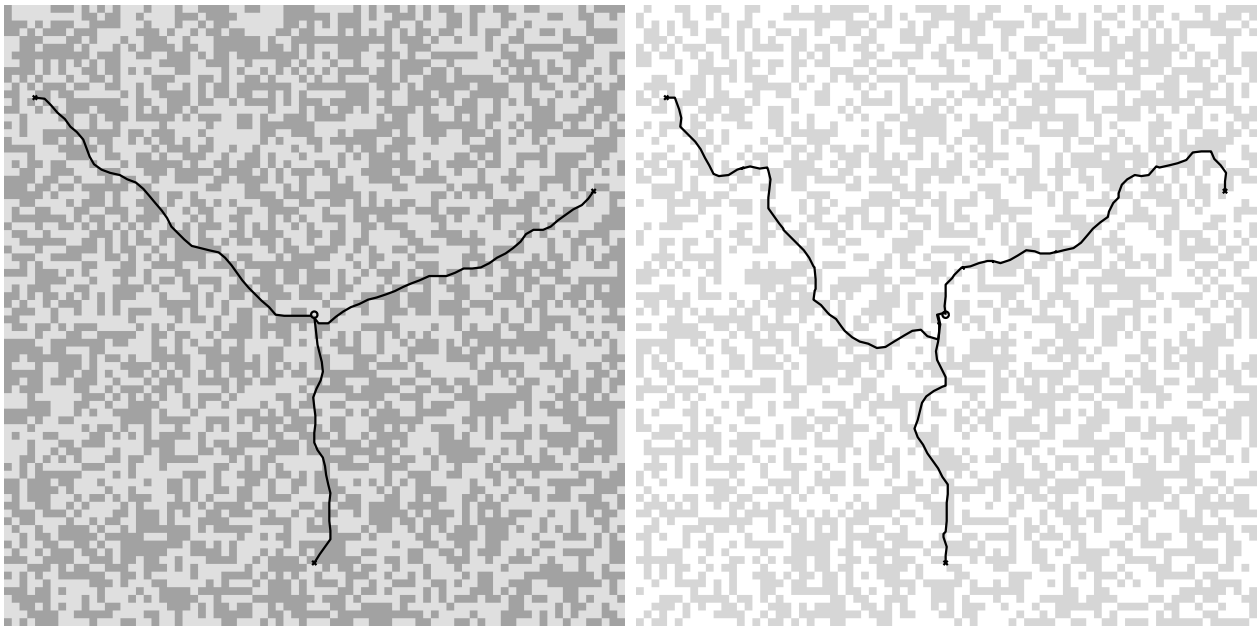
Figure 4: Optimal paths in a random media. The particle speed is $c_0 > 1$ `fig:randomPath` in the dark and 1 in the light region. Left: $c_0 = 2$. Right: $c_0 = 10$.

1.4. **Model problem: a toy three scale problem.** Consider a two dimensional material made up of fifty by fifty unit blocks. Each block is allowed to have a different periodic small scale structure. See Figure 5.

To solve the full three scale problem, we apply a two step procedure. First in each block, homogenize to get a homogenous material with a new
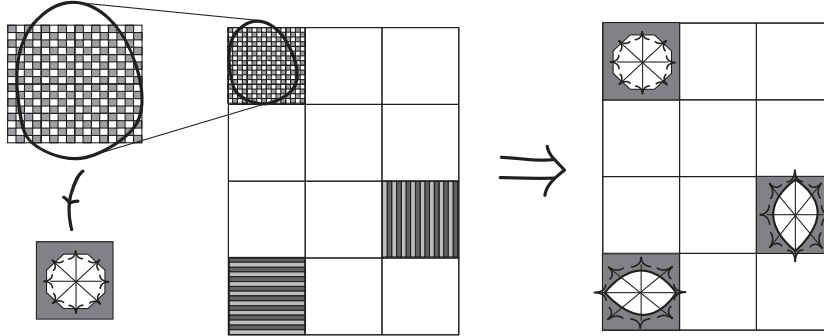
Figure 5: The three scale problem (left), result of homogenization in each medium scale cell (right)   `fig:3scaleSol`

(anisotropic) speed profile. Next, on the large scale, solve the front propagation problem on an grid which resolves each block, using the speed profile for the homogenized blocks. See Figure 5 and Figure 11. Accurate results can be obtained with a modest number of grid points on each block, see §5.2.

`sec:fronts`

2. Paths and fronts in an inhomogeneous medium

In this section we review front propagation in an inhomogeneous and anisotropic medium from the perspective of the optimal control theory. We discuss the least time perspective, and the related Eikonal equation for the distance.

We recall the derivation of the Hamilton-Jacobi equation for the distance function. The distance function is interpreted as the first arrival time for a front given as the envelope of particles moving along the optimal paths at speed given by c. The normal speed of a front is not the same as the particle speed. However, we make the observation in 2.8 that the particle speed function defines a norm, and that the HJ equation for the distance is a generalized eikonal equation in the *dual norm*.

These different interpretations of HJ equations are later used in section §3 to derive an efficient method for homogenization.

`sec:summary`

2.1. **Summary of notation and relationship between the variables.**
- x is a generic point in $\mathbb{R}^n$ representing position.
- p, q are generic vectors in $\mathbb{R}^n$ representing velocity.
- β is a generic vectors in $\mathbb{R}^n$ satisfying $|\beta| \leq 1$.
- α is a generic unit vector in $\mathbb{R}^n$ representing direction.
- $c(x, \alpha)$ is the particle speed in the direction α.
- $f(x, \alpha)$ gives the particle velocity in the direction α, $f(x, \alpha) = \alpha c(x, \alpha)$
- $F(x, n)$ gives the speed for a front with normal n.

- $b(x, q)$ is the cost at x to move with velocity q.
- The vectogram, $V_c(x) = \{f(x, \beta) \mid |\beta| \leq 1\}$ is a set of all permissible velocities at the point x.
- The Hamiltonian, $H(p, x) = |p|F(p/|p|, x)$.
- The Lagrangian $L(q, x) = 0$ if $q \in V_c(x)$, ∞ otherwise.

The normal speed F and particle speed c are related by the homogeneous Legendre Transform [23]. The Hamiltonian, H, and the Lagrangian L are related by the Legendre Transform, see section §2.5. The particle speed c and the metric cost function b are one sided inverse functions, see section §2.7. For each fixed x, the metric cost function b and the Hamiltonian H are norms on $\mathbb{R}^n$. The fact that these norms are dual is explained in section §2.8.

2.2. The speed function, vectograms.

Consider a medium which allows particle motion at limited speeds. Let x denote the position, and β denote the control value. Write $\dot{x}(s, \beta(s)) := \frac{d}{ds} x(s, \beta(s))$. The admissible paths $x(t, \beta(t))$ satisfy the controlled ordinary differential equation

| `dynamics` | (ODE) | $\dot{x}(s, \beta(s)) = f(x(s, \beta(s)), \beta(s))$ |

where $\beta(\cdot) \in \mathcal{B} := \{\beta(\cdot) : [0, \infty) \to \mathbb{R}^n, |\beta| \leq 1, \text{ measurable}\}$ is the *control*.

We restrict to the special case where the control is the choice of direction:

| `speedfunction` | (2) | $$f(x, \beta(s)) = c\left(x, \frac{\beta(s)}{|\beta(s)|}\right)\beta(s)$$ |

The *speed function* $c : \mathbb{R}^n \times \mathbb{S}^n \to [0, +\infty)$ gives the maximum speed allowed in the direction α, where $\alpha = \beta(s)|\beta(s)|^{-1}$ is a unit vector. We assume that c is convex in its second argument and satisfies the small-time controllability condition:

| `growth` | (3) | $0 < c_1 \leq c(x, \alpha) \leq C_1 < +\infty$ for every $x \in \mathbb{R}^n, |\alpha| = 1$. |

The function c is *homogeneous* if it is independent of x, $c(x, \alpha) = c(\alpha)$, *isotropic* if it is independent of the direction, α, $c(x, \alpha) = c(x)$, and *symmetric* if

| `speedsymmetric` | (4) | $c(x, -\alpha) = c(x, \alpha).$ |

We assume symmetry to ensure that the resulting distances on $\mathbb{R}^n$, $T_c(x_1, x_2)$, are symmetric, although the assumption can be dropped at the expense of some additional bookkeeping (some of the formulas will have minus signs in the velocities, see [23]).

For fixed $x \in \mathbb{R}^n$, the speed function c is a mapping of the unit sphere, $\mathbb{S}^n$, and also defines a *vectogram* $V_c \subset \mathbb{R}^n$:

$$V_c = \left\{ c\left(x, \frac{\beta(s)}{|\beta(s)|}\right)\beta \ \middle| \ |\beta| \leq 1 \right\}.$$

Vectograms [17] provide a simple way to illustrate the speed profile for each point x. See Figures 3 and 8.

sec:arrivaltime

2.3. **The arrival time function.** We can define a distance on $\mathbb{R}^n$ using the minimum time needed to move between two points along the admissible paths:

ds (5)
$$T_c(x_1, x_2) = \inf_{x(\cdot) \text{ admissible}} \{t \mid x(0) = x_1, x(t) = x_2\}.$$

It is easy to show that T_c defines a metric on R^n, where the symmetry property results from the fact that any admissible path from x_1 to x_2 can be retraced backwards taking the same amount of time (using (4)). The small-time controllability condition (3) can be used to show that the infimum is attained and that an optimal (not necessarily unique) control $\beta(s)$ actually exists. Moreover, since the goal is to minimize the time, it is clear that along any optimal path the particle should be moving with the maximum allowable speed for the current direction; i.e., $|\beta(s)| = 1$ and $f(x(s), \beta(s)) \in \partial V_c$ a.e. in $[0, t]$. Thus, the same distance function can be defined by using the class of admissible controls $\mathcal{A} := \{\alpha(\cdot) : [0, \infty) \to \mathbb{R}^n, |\alpha| = 1, \text{ measurable}\}$.

We define the time to reach the origin,

$$T(x) = T_c(x, 0).$$

In the special case where the speed function is homogeneous, $c(x, \alpha) = c(\alpha)$, the optimal paths are straight lines, and the arrival time is simply given by the ratio of the distance to the speed.

TimeHomog (6)
$$T(x) = \frac{|x|}{c(x/|x|)}, \quad \text{when } c(x, \alpha) = c(\alpha) \text{ is homogeneous.}$$

sec:dist

2.4. **The Hamilton-Jacobi equation.** The Hamiltonian is defined by

hjbdefn (7)
$$H(p, x) := \max_{\|\alpha\|=1} \{(p \cdot \alpha)c(x, \alpha)\}$$
$$= \|p\| F\left(\frac{p}{\|p\|}, x\right).$$

Here $F(n, x)$ is the normal speed of the front passing through the point x with outward unit normal n.

In this section we show directly that the first arrival time function satisfies the Hamilton-Jacobi equation, using the Dynamic Programming Principle [4]. Here we give a formal proof (assuming the solution remains smooth), for the reader's convenience, and to establish consistent notation. A rigorous treatment (using visosity solutions to handle the non-smoothness) as well as the proof of uniqueness for similar equations can be found in [14] and [4].

Lemma 1. The arrival time to the origin, $T(x)$, is a solution to the *Hamilton-Jacobi* equation

hjb (HJ)
$$H(\nabla T, x) = 1, \quad T(0) = 0$$

Proof. Assume that $T(x)$ is smooth and consider all paths, which start from x and move in the constant direction α for a small time h. Define $y_\alpha = x + hc(x, \alpha)\alpha$. Then

$$T(x) = \min_\alpha \{T(y_\alpha) + h + o(h)\}$$
$$= \min_\alpha \{T(x) + c(x, \alpha)\,(\alpha \cdot \nabla T(x)) + h + o(h)\}.$$

Subtracting $T(x)$, dividing by h, and taking the limit $h \to 0$ gives

$$-1 = \min_\alpha \{c(x, \alpha)\,(\alpha \cdot \nabla T(x))\}$$

or $\max_{|\alpha|=1} \{c(x, -\alpha)\,(\alpha \cdot \nabla T(x))\,s\} = 1$ as in (7), where we have used the symmetry of the speed (4). $\square$

The optimal particle trajectories are given by the characteristics of the Hamilton-Jacobi equation. If $c(x, \alpha) = c(x)$ is isotropic, then $H(p) = |p|c(x) = 1$, which is an Eikonal equation. In this case, the characteristic curves coincide with the gradient lines of the viscosity solution, yielding

$$n = \frac{\nabla T(x)}{|\nabla T(x)|} = -\alpha$$

and $F(x) = c(x)$. In the anisotropic case,

$$F(x, n) = \max_{\|\alpha\|=1} \{(n \cdot \alpha)\, c(x, -\alpha)\}.$$

2.5. The Lagrangian.
An equivalent was to define the distance, (5), is using the *Lagrangian*,

(8)
$$L(x, q) = \begin{cases} 0 & q \in V_c \\ \infty & \text{otherwise} \end{cases}$$

Then the definition of distance (5) can be rewritten as the Hopf-Lax formula [14] for the arrival time function

$$T(x) = \inf \left\{ t + \int_0^t L(x(s), \dot{x}(s))\, ds \;\middle|\; x(0) = 0, x(t) = x \right\}$$

where the infimum is over $W^{1,1}\,((0, t); \mathbb{R}^n)$. For consistency, we verify that the Hamiltonian $H(p, x)$ is obtained from the Lagrangian via the Legendre transformation [14]

$$H(x, p) = L^*(x, p) = \max_q \{p \cdot q - L(x, q)\}$$
$$= \max_{q \in V_c} \{p \cdot q\}$$
$$= \max_{|\alpha|=1} \{(p \cdot \alpha)\, c(x, \alpha)\}$$

sec:geodesic

2.6. **The geodesic distance.** We review the notion of geodesic distance in this context, and below we will relate it to Hamilton-Jacobi equations. The link between Hamilton-Jacobi equations and metrics has been observed before. We refer to [24] and the references therein.

We are given a metric cost function, $b(x, q)$ which is positively 1-homogeneous in the second variable,

1homogfc

$$(9) \qquad b(x, tq) = tb(x, q), \quad \text{for every } (x, q) \in \mathbb{R}^n \times \mathbb{R}^n \text{ and } t > 0$$

This will ensure that the distance defined below is invariant under re-parameterizations of the path. In addition, we assume that b is convex in the second variable and satisfies the growth condition:

growthfc

$$(10) \qquad c_2|q| \leq b(x, q) \leq C_2|q|, \quad \text{for every } (x, q) \in \mathbb{R}^n \times \mathbb{R}^n$$

with $0 < c_2 \leq C_2 < +\infty$. Under the assumptions (9) (10), the cost function defines a norm on $\mathbb{R}^n$, for each x,

Fcnorm

$$(11) \qquad \qquad \qquad \qquad \|q\|_{b(x)} = b(x, q)$$

We also assume that $b(x, q) = b(x, -q)$, which ensures the distance is symmetric, $d_b(x_1, x_2) = d_b(x_2, x_1)$.

Given a path $x(\cdot) \in W^{1,1}((0, t); \mathbb{R}^n)$, the total cost of the path is

Jdefn

$$(12) \qquad \qquad J[x(\cdot)] = \int_0^t b\left(x(s), \dot{x}(s)\right) \, ds$$

The geodesic distance between two points is the minimal cost

geodesic

$$(13) \qquad \qquad d_b(x_1, x_2) = \inf_{x(0)=x_1, x(t)=x_2} J[x(\cdot)]$$

where the infimum is over $x(\cdot) \in W^{1,1}((0, t); \mathbb{R}^n)$. Using the growth condidtion, it is easy to show that the above infimum will actually be attained along some optimal path.

Remark (Riemannian and Finslerian metrics). If the cost function is given by the square root of a convex quadratic function, i.e.

$$b(x, \alpha) = \sqrt{g_{ij}(x)\alpha_i\alpha_j}$$

for $g(x)$ a symmetric positive definite matrix, the resulting metric, d_b, is Riemannian. (In that case the vectograms V_c are ellipses.) Otherwise, d_b is a *Finslerian* metric [24]. In a Finslerian metric, geodesics need not be differentiable, as is the case for the octagon norm. Since the viscosity solution theory allows for this type of weak solutions, we are able to compute distances in the more general metric. See [9][3] for more information on Finslerian metrics.

`sec:relating`

2.7. **Relating the geodesic metric and the arrival time.** So far we have defined two distances. The arrival time, $T_c(x_1, x_2)$, (5), is the arrival time using paths which move at speed admissible by the speed function $c(x, \alpha)$. The geodesic distance $d_b(x_1, x_2)$ (13) is the minimal cost of paths, where the cost is measure using the metric cost function $b(x, p)$. The two distances are equal if the metric cost function and the particle speed function are (one-sided) inverses.

Lemma 2. The distances T_c and d_b defined by (5) and (13), respectively are equal, provided that the speed function, c, and the cost function, b, are related by

`fcdefn`   (14) $b(x, c(x, \alpha)\alpha) = 1, \quad$ for all $|\alpha| = 1, x \in \mathbb{R}^n$

with the remaining values of b determined by homogeneity (9).

Proof. We argue formally, assuming the infimum in the definitions is achieved by differentiable paths. The proof can be made rigorous by approximation. Given $x_1, x_2 \in \mathbb{R}^n$, suppose $T_c(x_1, x_2) = t$ and $d_b(x_1, x_2) = s$.
    First let

$$x(\cdot) : [0, t] \to \mathbb{R}^n, \quad x(0) = x_0, \ x(t) = x_1.$$

be an admissible curve for the speed function c. Then $x(\cdot)$ satisfies (ODE), and $T_c(x_0, x_1) = t$. Compute the integral in the definition (13) using the path $x(\cdot)$. Then by (ODE), $\dot{x}(s) \in V_c$. Furthermore, we can assume that $\dot{x}(s) \in \partial V_c$, since otherwise the curve could be made faster. Thus by (14), $b(x, \dot{x}) = 1$, so $s \le t$.
    Next let $x(\cdot)$ be a curve from x_1 to x_2 for which the cost $J[x(\cdot)] = s$. We can find a parameterization of the path by arclength, i.e. a path $y(\cdot)$, for which $b(y(s), \dot{y}(s)) = 1$. Then by (14), $\dot{y}(s) \in V_c$, the vectogram at $y(s)$, so $y(\cdot)$ is an admissible path for the distance function T_c. Thus $t \le s$. $\square$

A similar proof of this property can be also found in [25].

`sec:dualnorm`

2.8. **Dual Norms, The Eikonal equation.** We show that (HJ) can be rewritten as an Eikonal equation in a suitable norm. This relates the speed or cost functions to the normal velocity.
    We refer to [6][Appendix 1.1.6] for material on norms and dual norms. Given a closed, bounded set with non-empty interior, e.g. V_c, it can be used to define a norm (by using the set as the norm ball and extending by homogeneity) provided the set is symmetric about the origin, and convex. Convexity of the set ensures the triangle inequality for the norm.
    Given a norm $\| \cdot \|$ on $\mathbb{R}^n$, the dual norm $\| \cdot \|_*$ is defined as

`dualnorm`   (15) $\|p\|_* = \max\{q \cdot p \mid \|q\| = 1\}$

Then $\|p\|_{**} = \|p\|$.

Example. The $\| \cdot \|_p$ norms are dual to the p^* norms, with $1/p + 1/p^* = 1$ for $1 \le p \le \infty$. In particular this is true for $p = 1$ and $p = \infty$, where the norm balls are diamonds and squares. Generalizing this case, dual polygonal norms can be obtained as well.

Write, for fixed x, the dual norm

$$\|p\|_{b^*(x)} := \max\{p \cdot q \mid \|q\|_{b(x)} = 1\}$$
$$= \max_{\|q\|=1}\{p \cdot q \, c(x,p)\}.$$

by (14). Thus (HJ), (7) are equivalent to

anieik	(Eikonal)

$$\|\nabla u(x)\|_{b^*(x)} = 1.$$

Conversely, if we are given the Hamilton-Jacobi equation $H(p,x)$ which is positive 1-homogeneous in p for each x, we can recover the cost function by again taking the dual

fcfromH	(16)	$\|p\|_{b(x)} = \max\{q \cdot p \mid H(p,x) = 1\}.$

Conversely, the Legendre transform of the norm $\| \cdot \|_{b^*(x)}$ is the dual norm unit ball [6][pg 93], which gives the vectogram.

Remark. In general it is not true that homogenizing and squaring commute. The reason that the results of [10] (for eikonal squared) and [11] (for eikonal) give equivalent homogenized values, is that the Legendre transform of a norm is the indicator set of the dual norm, while the Legendre transform of a norm squared is the dual norm squared (see [6] example 3.26 and 3.27).

3. Main Homogenization Result

sec:homog

3.1. Homogenization background.

Theoretical works on homogenization provide existence results, and convergence rates for the solution homogenization problem. We mention the early unpublished work [19] for Hamilton-Jacobi equations, and refer to the textbooks, [20] for linear equations, and [7], for homogenization of HJ equations and Riemannian metrics [pp142–145]. A list of more detailed references can be found in the review [13]

Explicit analytic solutions for several examples can be found in [10]. A series of examples in the time dependent front propagation case, can be found in [11]. Both works find explicit solutions by homogenizing the Lagrangian see sections §3.4 and §2.5. The first work used Hamiltonians which are homogeneous order two in p, $(H(p,x)^2$ in our notation), and so the resulting Lagrangian was also homogeneous order two in p. The second work used a time-dependent equation, with a similar Hamiltonian to the one herein. In both cases, the Lagrangian is related to the Hamiltonian by the Legendre transform.

The cell problem (section §3.3) can be solved numerically to compute $\bar{H}(p)$. This was done for front propagation in [18], and for more general Hamiltonians in [21] and [22]. There are other methods for computing $\bar{H}(P)$, see [15].

3.2. Homogenization in one dimension.

Example. For the case of front propagation in a one-dimensional periodic medium, it is not difficult to show that the homogenized speed function is the harmonic mean of the speed function over a periodic cell. Suppose our one dimensional domain consists of ϵ-intervals with the speed alternating between 1 and 5. Then the travel times in these materials are 1 and $1/5$, so the total time to for the front to traverse the entire domain is $3/5$, and the average speed is $5/3$, the harmonic mean of 1 and 5.

To obtain this result formally for the Hamilton-Jacobi equation, we go through the following procedure. (i) rewrite $c(x)|u_x| = 1$, as $|u_x| = c(x)^{-1}$, (ii) average the reciprocal of the speed function (iii) divide by the averaged coefficient, to obtain

$$\frac{1}{\text{average of } c(x)^{-1}} |u_x| = 1$$

Remark. This heuristic is quite similar to the one used when homogenizing linear equations, but it is not directly applicable to HJ equations in higher dimensions. To obtain the total cost to travel from x_0 to x_1 the cost is integrated along the optimal trajectory, (which need not be a straight line) and then divided by $|x_0 - x_1|$. The cost has units of inverse speed, the average cost is the time divided by the distance.

sec:cell

3.3. The cell problem for Hamilton-Jacobi equations. In this section we outline the cell problem. A precise statement of a typical theorem can be found, for example, in [8], or in the review [13]. For a reference medium which is periodic on the cube $[-1, 1)^n$, write

HJe   (HJ$^\epsilon$)
$$H\left(\nabla u^\epsilon, \frac{x}{\epsilon}\right) = 1,$$

for the Hamiltonian with periodicity ϵ. The boundary conditions are

$$u^\epsilon(0) = 0,$$

or more generally $u^\epsilon(x) = 0$ for x in the target set Γ.

The cell problem is derived using a formal asymptotic expansion, typical examples of which can be found in Chapter 5 of [16]. If we are interested in the limit $\epsilon \to 0$, we can formally expand the solution u^ϵ analytically in ϵ, to write $u(x) = u^0(x, x/\epsilon) + \epsilon u^1(x, x/\epsilon) + o(\epsilon)$. Additional arguments which we skip show that we can assume

$$u^\epsilon(x) = u^0(x) + \epsilon u^1(x/\epsilon) + o(\epsilon).$$

Inserting the expansion into the equation, and collecting terms of $O(1)$ gives

$$H\left(\nabla_x u^0 + \nabla_y u^1, y\right) = 1,$$

where $y = x/\epsilon$. The variable in this last equation is y, so $\nabla_x u^0 = p$, an unknown constant. The left hand side of the previous equation is a function of y, while the right hand side is constant. Thus we have a solvability

condition: we need to find a periodic function $v(y)$, and a vector p which solve the cell problem

$$H(p + \nabla v, x) = 1.$$

Then we can define

$$\bar{H}(p) = 1$$

for that p, and extend $\bar{H}$ to other values along the line $q = tp$ by homogeneity.

The homogenization theorem says that u^ϵ converges (uniformly on compact subsets, possibly with a rate) to the solution of

$$\bar{H}(Du) = 1.$$

sec:var_fronts

3.4. **Variational formulation for fronts.** For time-dependent fronts, a variational formulation of the homogenization problem was used in [11]. This is based on the Lagrangian formulation of the problem, and the convergence is in the sense of Γ-convergence [7]. They solved a problem of the form

$$\bar{L}(q) = \liminf_{T \to \infty} \frac{1}{T} \inf_{\phi \in H_0^1(0,T)} \int_0^T L(qt + \phi(t), q + \dot{\phi}(t)) \, dt$$

In this case, the minimization is performed for each value of q, and the Hamiltonian $\bar{H}(p)$ is recovered via the Legendre transform. The resulting Hamiltonian is homogeneous of order one in the gradient, and the Lagrangian is a characteristic function, as in (8). We note that the discontinuous nature of the Lagrangian limits the usefulness of this approach for numerical approximation.

sec:homogmetric

3.5. **Homogenization of metrics.** In this section, we review a homogenization result for the geodesic distance functional.

We use the result from [2]. Consider the metric const functional (12). In this section, we also assume that $b(\cdot, q)$ is $[-1, 1)^n$ periodic for every $q \in \mathbb{R}^n$. Then for every $\epsilon > 0$, set

$$J_\epsilon[x(\cdot)] = \int_0^t b\left(\frac{x(s)}{\epsilon}, \dot{x}(s)\right) ds,$$

According to the theorem from [2], J_ϵ Γ-converges on $W^{1,1}((0,t); \mathbb{R}^n)$ (in the L^1-topology) to the function defined by

$$J[x(\cdot)] = \int_0^t \bar{b}(\dot{x}(s)) \, ds$$

Here $\bar{b} : \mathbb{R}^n \to [0, +\infty)$ is 1-homogeneous convex function which also satisfies (10) and is given by

barf   (17) $$\bar{b}(q) = \lim_{\epsilon \to 0^+} \inf_{x(\cdot)} \left\{ \int_0^t b\left(\frac{x(s)}{\epsilon}, \dot{x}(s)\right) ds \mid x(0) = 0, x(t) = q \right\}$$

where again the infimum is over $x(\cdot) \in W^{1,1}((0,t); \mathbb{R}^n)$.
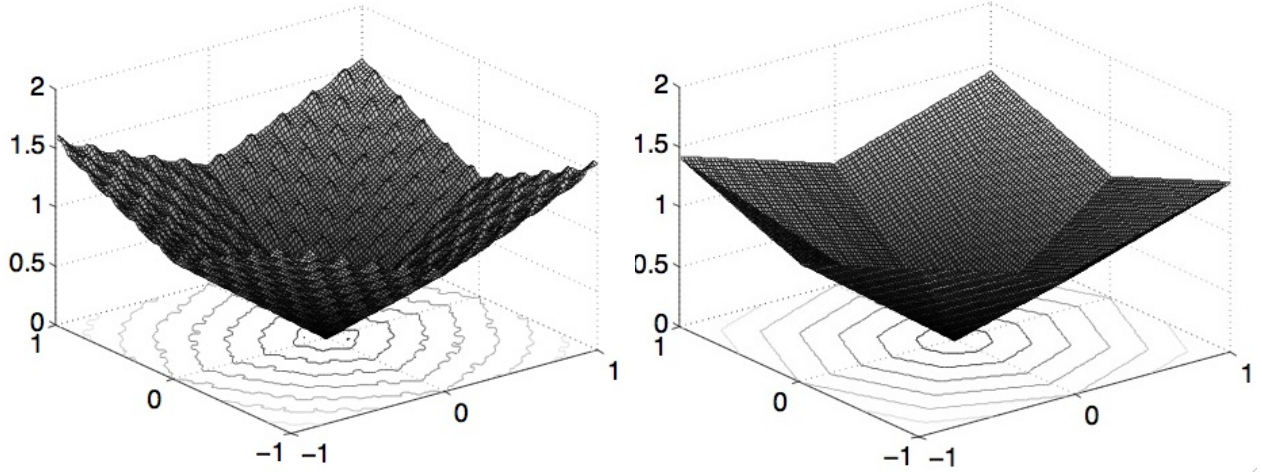
Figure 6: The arrival time $T^\epsilon(x)$ using the periodic cost function $b(x/\epsilon, p)$ converges to the arrival time $T(x)$ with the homogenized cost $\bar{b}(p)$. As a result, the homogenized cost can be estimated from the arrival time $T^\epsilon(x)$.　`fig:cones`

3.6. **Main Homogenization Result.** While the formula (17) requires the solution of a path minimization problem for each direction q, we can convert the problem to single eikonal equation (Eikonal) which whose solution, the homogenized distance function, can by used to record the homogenized speed from the relation (19). This results in an efficient method for $\bar{H}(p)$ using the relation (7). We record this result in Theorem 1. See Figure 6 for an illustration of the result, taken from a computation.

Definition 1. The Hamiltonian $H(p, x) : \mathbb{R}^n \times \mathbb{R}^n \to \mathbb{R}$ is a *metric* or *generalized eikonal* Hamiltonian if for each fixed x, $H(\cdot, x) : \mathbb{R}^n \to \mathbb{R}$ satisfies the following

$$H(\cdot, x) \text{ is convex}$$
$$H(tp, x) = tH(p, x) \text{ for all } t \geq 0$$
$$c|p| \leq H(p, x) \leq C|p| \text{ for all } |p| = 1$$

with $0 < c_2 \leq C_2 < +\infty$.

Definition 2. The Hamiltonian $H(p, x)$, which is periodic on the cube $x \in [-1, 1)^n$ *homogenizes* to $\bar{H}(p)$ if the viscosity solutions $T^\epsilon(x)$ of the Hamilton-Jacobi equation (HJ$^\epsilon$) with $T^\epsilon(0) = 0$ converge uniformly on compact subsets to the viscosity solution $T(x)$ of $\bar{H}(\nabla T) = 1$, with $T(0) = 0$.

`thm:HJ`　**Theorem 1.** *Let $H(p, x)$ be a metric Hamiltonian which is periodic on the unit cube. The $H(p, x)$ defines a distance on $\mathbb{R}^n$. We can write*

$$H(p, x) = \|p\|_{b(x)^*}$$

where $b(x, p)$ is corresponding metric cost function. Then $H(p, x)$ homogenizes to $\bar{H}(p)$ which is a homogeneous metric Hamiltonian. Furthermore

$$\bar{H}(p) = \|p\|_{\bar{b}^*} \tag{18}$$

HJbar

which is the dual norm (15) of the $\bar{b}$ norm. The values can be obtained from

$$\bar{b}(p) = \frac{1}{\bar{c}(p)} = \frac{T(p)}{|p|} = \lim_{\epsilon \to 0} \frac{T^\epsilon(p)}{|p|} \tag{19}$$

fcbar

where T^ϵ is the solution of (HJ^ϵ).

So we can solve one finite ϵ eikonal equation, and approximate all of $\bar{H}(p)$ using that solution.

Proof. This result is obtained from translating freely between the various formulations of the front propagation problems, as summarized in §2.1 and as explained in the earlier sections.

Since $H(p, x)$ is a metric Hamiltonian, we can recover the cost function $b(x, p)$ from the Hamiltonian using the dual norm formula (16).

By the results of §2.3, the solution $T^\epsilon(x)$ of the Hamilton-Jacobi equation (HJ^ϵ) is the arrival time from the origin using admissible speeds c. But this is equivalent, using §2.7, to the distance in the b^ϵ metric. Using the convergence result for metrics, §3.5, this cost function converges to a cost function $\bar{b}(p)$, which is also homogeneous of order one. Using the equivalence of §2.7 again, the resulting Hamiltonian

$$\bar{H}(p) = \|p\|_{\bar{b}^*}$$

can be written as the dual norm to the homogenized cost function $\bar{b}$, as in (Eikonal).

Finally, the solutions T of (18) along with $T(0) = 0$ are given by the time to reach the point x, where the cost to move in the direction α is $\bar{b}(\alpha) = 1/\bar{c}(\alpha)$. Since these functions are convex, the optimal path is a straight line, in the directions $\alpha = x/|x|$. Then the travel time for a particle is simply the distance over the particle speed (6)

$$T(x) = \frac{|x|}{\bar{c}(x/|x|)}$$

which gives the second equality in (19). The last equality in (19) follows from the convergence result for the solutions of the finite ϵ problems.   □

Remark (Convergence rate). The result of [8], which applies if we use the *Kruzkov transformation*: $T^\epsilon(x) = -\log(1 - v^\epsilon(x))$ gives a convergence rate $T(x) = T^\epsilon(x) + O(\epsilon)$. The result is useful computationally, because we can use Richardson extrapolation in ϵ to better approximate $T(x)$.

4. The Numerical Method

In this section we present the numerical method. To compute the homogenized speed function, using the results of §3, we can simply compute a distance function to the origin by solving (HJ$^\epsilon$). The speed function is related to an eikonal equation by the results of §2.

The equation (HJ$^\epsilon$) can be solved by standard methods. Then using (19) we obtain approximations to the values $\bar{b}(\alpha)$ for a discrete set of directions α.

There are two main approaches to solving the homogenized equation (18). The first is a simple, low accuracy approach. Compute $\bar{b}(\alpha)$ for directions on the grid, and then solve the resulting problem as a discrete shortest path problem on a graph, using Dijkstra's method. The second approach is accurate, but requires more sophisticated algorithms. Solve the isotropic problem (18). For this the values of $\bar{b}(\alpha)$ are needed for every direction α, and an isotropic Hamilton-Jacobi solver is also needed. To this end, intermediate values of $\bar{f}(\alpha)$ can be obtained by interpolation: we use second order ENO interpolation, which was suitable for piecewise quadratic functions, periodic on $[0, 2\pi]$. Then the ordered upwind method [23] can be used to solve the equation.

The three scale problem can be solve using a piecewise constant norm in each unit cell, or by interpolating the norm across cells.

The complete algorithm consists of two phases: the first phase is to compute the homogenized speed function $c(\alpha)$ for all $\alpha \in \mathbb{S}^2$ and the second is to solve for $T(x)$.

4.1. **Computing the homogenized speed function.** First (A1), compute an approximation to $\bar{c}$ by solving an eikonal equation for finite ϵ. In terms of the vectogram, (A2) approximates $U_{c(\alpha)}$ for a discrete set of directions α_i and (A3) interpolates these points.

- INPUT: speed function $c^\epsilon(x, \alpha)$.
- OUTPUT: $\bar{c}(\alpha)$, the approximation to the homogenized speed.

(A1) Choose $0 \ll h \ll \epsilon \ll 1$. Numerically solve

$$(20) \qquad \sup_{\|\alpha\|=1} \{c(x/\epsilon, \alpha)\alpha \cdot \nabla T^\epsilon(x)\} = 1$$

$$(21) \qquad\qquad\qquad T^\epsilon(0) = 0,$$

  using a finite difference method on a uniform cartesian grid on $Q = [-1, 1]^2$ with spatial resolution h.

(A2) Choose k vectors, $\{q_i\}$, $i = 1, \ldots k$ which lie on the grid and are of length close to unity. Approximate $\bar{b}$ on the grid directions, using (19)

$$\bar{b}\left(\alpha_i = \frac{q_i}{|q_i|}\right) := \frac{T^\epsilon(q_i)}{|q_i|}, \quad i = 1, ..., k.$$

(A3) Interpolate the values $\{\bar{b}(\alpha_i)\}$, $i = 1, \ldots k$ to approximate $\bar{f}(\alpha)$ for all $\alpha \in \mathbb{S}^n$.

4.2. **Solving the homogenized equation on a graph.** We implement a discrete analogue of the dynamic programming principle, where the optimal path is approximated by piecewise linear paths on a finite set of nodes in Ω. We embed a network N in Ω consisting of a finite node set $V \subset \Omega$ and weighted directed edges $E \subset V \times V$. For each $x \in V$, the neighbors of x is the set

$$\mathcal{N}(x) = \{y \in V : (x, y) \in E\}.$$

We call the set

$$\mathcal{C}(x) = \{y - x : y \in \mathcal{N}(x)\},$$

the *local connectivity* of N at $x \in V$. Construct N so that for all $x, y \in V$

$$y \in \mathcal{N}(x) \Leftrightarrow x \in \mathcal{N}(y)$$

and generally,

$$|v| \text{ is small for all } v \in \mathcal{C}(x), x \in V.$$

The latter condition allows for more accurate approximation of the optimal trajectories (and consequently of the value function) by piecewise linear paths. Naturally, the metric between two adjacent nodes are assigned as the (directed) edge weights. The shortest path problem on a network can then be efficiently solved using, say, Dijkstra's algorithm or the fast sweeping method.

- INPUT: $\bar{f}(\alpha)$ from phase one of the algorithm.
- OUTPUT: $\tilde{u}$, the discrete approximation to the $u(x)$ defined on V.

(B1) For each $e_i = (x, y) \in E$ assign an edge weight

$$w_i = d(x, y) = |y - x|/\bar{c}\left(\frac{y - x}{|y - x|}\right).$$

(B2) Let $\tilde{u}^0$ the value function defined on V. Set

$$
\begin{aligned}
\tilde{u}^0(x) &= 0 \quad \text{if } x \in V \cup \Gamma, \text{ and} \\
\tilde{u}^0(x) &= \infty \quad \text{if } x \in V \backslash \Gamma.
\end{aligned}
$$

(B3) Solve the shortest path problem on N using Dijkstra's algorithm where $\tilde{u}^0(x)$ is the least cost to travel from $V \cup \Gamma$ to $x \in V$ in N.

Choice of grid directions q_i and network N. Using Dijkstra's algorithm (B1) - (B3) to approximate the value function, step (A3) may be omitted by carefully choosing the grid directions q_i (in (A2)) and network N.

Consider the network where the vertices V are given by uniform cartesian discretization of Ω with refinement h, and for each interior node, the neighbors are the eight closest nodes,

$$\mathcal{C} = \mathcal{C}(x) = \{(\pm h, 0), (\pm h, \pm h), (0, \pm h)\}.$$

Then by choosing the grid directions q_i to be

$$q_i = v_i/h \text{ where } v_i \in \mathcal{C}, i = 1, ..., 8$$

we can avoid the interpolation step (A3), since the values at the grid directions are the only values needed to compute the weights in (B1).

However, this introduces an additional error, because the paths used for computing the metric in (17) are being restricted to those which are piecewise linear with slopes corresponding to the grid directions. This error can be reduced by using more grid directions.

4.3. **ENO interpolation for step (A3).** We use a second-order essentially non-oscillatory (ENO) method for interpolation. The ENO method is accurate for piecewise quadratic functions, which may have corners. This class matches the shape of the vectograms corresponding to the homogenized speed functions. See Figure 7.
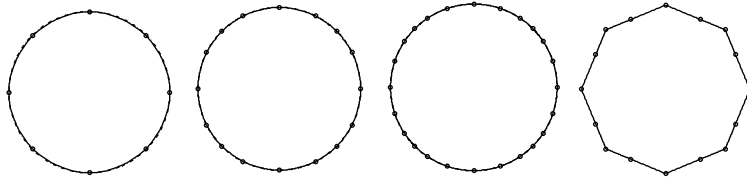

Figure 7: Interpolation using ENO. Interpolated circle, using 8, 16, and 24 points. Interpolated octagon using 16 points.   `fig:ENOcircle`

Steps (B1) - (B3) only use a discrete set of directions $\tilde{f}_0(\alpha_i)$. For methods that exploit $\tilde{f}_0(\alpha)$ for all $\alpha \in S^2$, the accuracy of the interpolation step in (A3) directly affects the accuracy of the approximated value function $\tilde{u}^0$. The solution obtained by (B1) - (B3) can be viewed as an approximation using linear interpolation in (A3).

Better, we propose to apply a second-order essentially non-oscillatory (ENO) method for interpolation. The ENO method is suitable for general (as opposed to Riemannian) metrics as it is capable of capturing piecewise linear and quadratic functions.

Assume that the unit vectors $\{\alpha_i\}$ are ordered in (counter-clockwise) direction. Suppose we wish to interpolate $\{\tilde{f}_0(\alpha_i)\alpha_i\}$ between $i = j$ and $j+1$. The second order ENO method works as follows. Denote x_i, y_i to be the x and y coordinates for $\tilde{f}_0(\alpha_i)\alpha_i$, respectively. We describe the case where x_i is the independent variable, which should be applied where $|x_j - x_{j+1}|$ is not too small. The case where y_i is the independent variable follows similarly, where $|y_j - y_{j+1}|$ is not too small.

Step 1 Find the interpolating quadratics

$$h_1(x) = a_1 x^2 + a_2 x + a_3, \qquad h(x_i) = y_i, \qquad i = j-1, j, j+1,$$
$$h_2(X) = b_1 x^2 + b_2 x + b_3, \qquad h(xi) = y_i, \qquad i = j, j+1, j+2$$

Step 2 If $a_1 < b_1$, choose $h_1(\alpha)$ as the interpolating function between $\tilde{f}_0(\alpha_j)\alpha_j$ and $\tilde{f}_0(\alpha_{j+1})\alpha_{j+1}$. Otherwise, choose $h_2(\alpha)$ as the interpolating function.

Higher order ENO interpolation can be implemented similarly, by considering higher order interpolation polynomials on more directions.

multiple

4.4. Extension to the three scale problem.

Our algorithm generalizes naturally to problems with multiple regions, each with different periodic structure. Suppose $\Omega = \bigcup_i \Omega_i$ is a (finite) partition of the domain, where each Ω_i is equipped with a speed function $f_\epsilon^i(x, \alpha)$. By repeating (A1) - (A3) in each domain, we approximate $\bar{f}^i(\alpha)$ for each i. Define the piecewise constant (in x) speed function on Ω by

$$\bar{f}(x, \alpha) = \bar{f}^i(\alpha), \quad x \in \Omega_i,$$

Then the second phase proceeds as before with the weights assigned as in (B1) using the globally defined speed function $\bar{f}(x, \alpha)$.

5. NUMERICAL RESULTS

sec:numericalresults

Numerical results and validation are presented in this section. We present homogenization results for various speed functions f_ϵ for which an analytic solution is known. The methods and parameters used in our implementation are described. We numerically validate the first order convergence in ϵ. Finally, we present a result for the three scale problem.

homof

5.1. Homogenized speed functions.

In this section computed homogenized speed functions for homogeneous periodic materials, with speed 1 and 2.

Analytical values of $\bar{H}(p)$ given various $c(x)$ can be found in [11] [10].

We compared numerically our computed values $\bar{b}$ with the analytical values of $\bar{H}(p)$ by performing the dual norm calculation numerically numerically using (16)

$$\|q\|_{\bar{b}} = \sup_{|p|=1} \{q \cdot p \mid \bar{H}(p) = 1\}$$

over a discrete set of unit vectors. For visualization purposes we display vectorgrams which are obtained trivially from $\bar{b}$.

A full description of the checkerboard example can be found in [1].

All the speed functions are function defined on $[-1, 1]^2$ and extended periodically. The numerically computed homogenized vectograms are shown in Figure 8, overlaid on the exact result. We also compared the error for a fixed pattern (checkerboard or stripes) but different speed ratios c in the material. The error was computed for a fixed directions as a function of c, and also as a function of the direction for fixed c. See Figures 9 and 10.
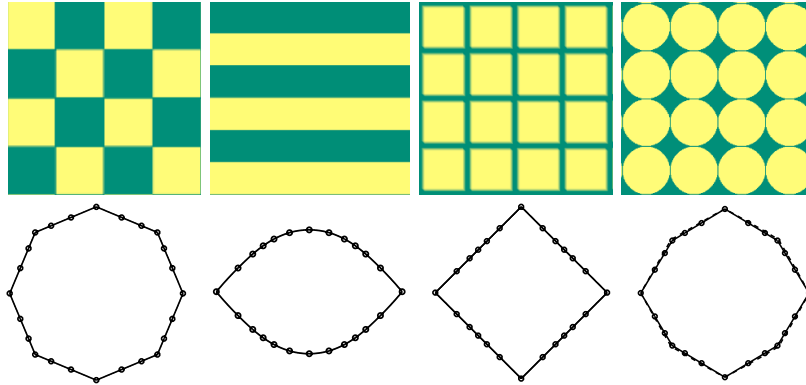
Figure 8: Period domains and computed vectograms: checkerboard, stripes, `fig:vectograms` squares, and circles.

Example (checkerboard).

$$c^{ch}(x,y) = \begin{cases} c_0 & xy \geq 0 \\ 1 & \text{otherwise} \end{cases}$$

The exact solution is an octagon for $c_0 \geq c_0^*$,

$$\bar{H}(p_1, p_2) = \frac{c_0}{(\sqrt{2}-1)\min(|p_1|, |p_2|) + \max(|p_1|, |p_2|)}, \quad c_0 \geq c_0^*$$

and for $c_0 \in [1, c_0^*]$ the solution interpolates between a circle and an octagon, [1]. The plot is for $c_0 = 2$.

Example (Stripes).

$$c^{st}(x) = \begin{cases} 1 & x_2 \in [0,1) \\ 2 & \text{otherwise} \end{cases}$$

The exact solution for general stripes pattern can be found in [11]. In this case there is no closed formula for $\bar{H}$ however the stripes can all be lines up and the optimal path for this configuration can be found by solving for the optimal angle, which results in Snell's law of refraction.

Example (Squares).

$$c^{sq}(x) = \begin{cases} 1 & x_1 = 0 \text{ or } x_2 = 0 \\ 1/2 & \text{otherwise} \end{cases}$$

The exact solution is readily seen to be given by a diamond shaped vectogram, since the optimal paths move only in the vertical and horizontal directions.

circle   *Example* (Circles).

$$c^{cir}(x) = \begin{cases} 1 & \|x\| \leq 1 \\ 2 & \text{otherwise} \end{cases}$$

The exact solution is in [10] [11], optimal paths take are vertical, horizontal, or quarter circles.

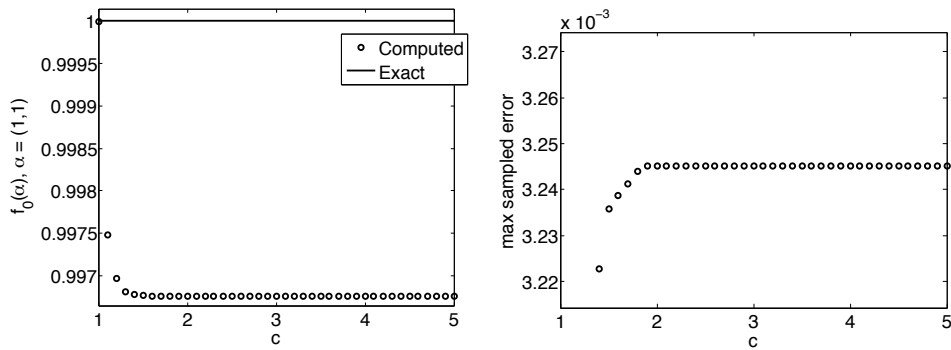$$\bar{H}(p_1, p_2) = \max\left\{ |p_1|, |p_2|, \frac{2}{\pi}(|p_1| + |p_2|) \right\}$$

Figure 9: Results using the checkerboard pattern for speeds in $\in [1,5]$. Left: fig:varyChecker
$\bar{c}(\alpha)$ for $\alpha = (1,1)$. Right: maximum error over all sampled directions.
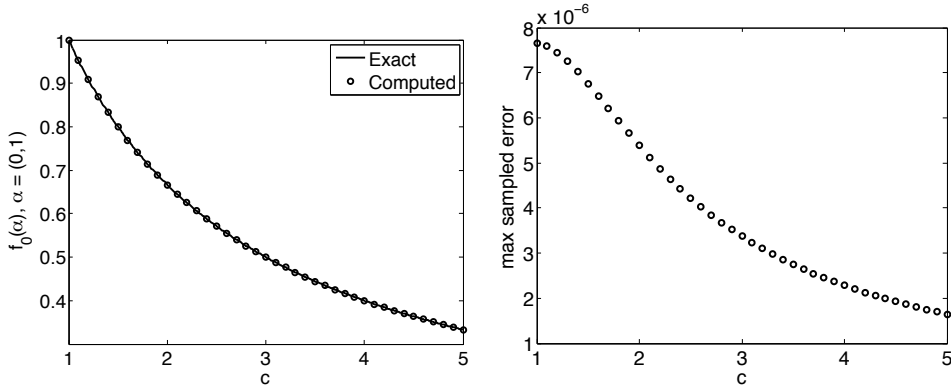

Figure 10: Results using the horizontal stripes pattern for various speed in   fig:varyHorizontal
$[1,5]$. Left: $\bar{c}(\alpha)$ for the direction $\alpha = (0,1)$. Right: maximum error over all sampled directions.

5.2. **The toy three scale problem.** In this section we consider the model problem from §1.4. Consider the following speed function:

$$c(x) = \begin{cases} c^{ch}(x) & \text{for } x \in [-1, -\frac{1}{3}]^2 \cup [-\frac{1}{3}, \frac{1}{3}]^2 \cup [\frac{1}{3}, 1]^2 \\ c^{st}(x) & \text{for } x \in [-1, -\frac{1}{3}] \times [-\frac{1}{3}, \frac{1}{3}] \cup [-\frac{1}{3}, \frac{1}{3}] \times [\frac{1}{3}, 1] \\ c^{vert}(x) & \text{for } x \in [-\frac{1}{3}, \frac{1}{3}] \times [-1, -\frac{1}{3}] \cup [\frac{1}{3}, 1] \times [-\frac{1}{3}, \frac{1}{3}] \\ c^{sq}(x) & \text{otherwise} \end{cases}$$

where c^{vert} is the horizontal stripes c^{st} rotated by 90 degrees. We solve for $u^0(x)$ in (20),(21), in $[-1, 1]^2$ with starting point $(-0.7, -0.7)$. The numerically computed homogenized value function is shown in Figure 11.
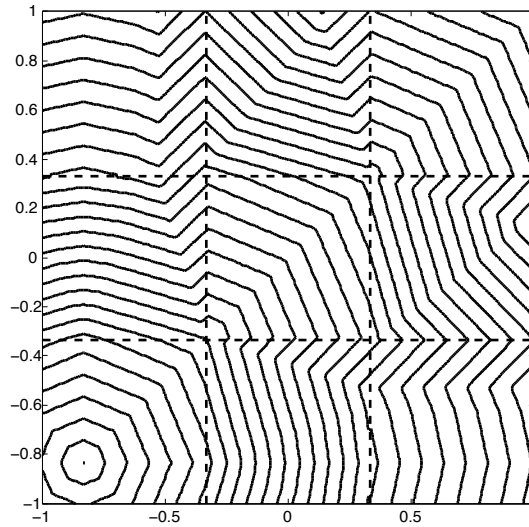

Figure 11: Level sets of the homogenized solution $T(x)$. The dotted lines are the interfaces where the periodic pattern changes.   threeScaleProb

5.3. **Methods and parameters used.** We used the first order fast marching method to solve the boundary value problem (20), (21) in A1. for grid size $n = 1200$ and 2400 (so the refinements are h = 1/600 and 1/1200). Then we applied Richardson's extrapolation on h, the spatial resolution, to obtain second order accuracy. The grid directions $\{q_i\}$ were chosen to be the 24 directions on a 7×7 stencil, see Figure 12. Subsequently, for (B1) - (B3), the local connectivities of the uniformly cartesian network N were:

$$\mathcal{C} = \{(ah, bh) : a, b \in \{0, \pm 1, \pm 2, \pm 3\}\}.$$

The shortest path problem on N was computed using the fast sweeping method.
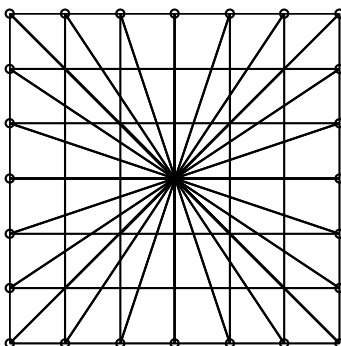
Figure 12: The grid directions $\{q_i\}$.

`fig:24direction`

The main script was written in Matlab, and the fast marching method was implemented in C, using code downloaded from [5]. The computations took a few seconds on a desktop computer. The default ration of fast and slow speed in the cells was 2.

`justifyextrap`

5.4. **Cell and domain resolutions.** In practice, computations were performed for finite values of ϵ. More accurate numerical results were obtained by using Richardson extrapolation for two small values of ϵ. In this situation, there is a trade off between the number of periodic cells on the domain, and the number of grid points in each cell.

We found that accurate results could be obtained by resolving each periodic cell very well, even if a relatively small number of cells were used. Finally, we extrapolated in the spatial resolution h as well. Table 1 compares the error using different extrapolation choices. Extrapolation in both parameters yields the best accuracy.

Given n (n^2 is the number of grid points used in step (A1).), and ϵ, define the *cell refinement* by

$$n_\epsilon := n\epsilon.$$

The accuracy of our algorithm depends on two parameters: ϵ and n_ϵ. We observed that the convergence rate depends more strongly on n_ϵ, than on ϵ.

Figure 13 shows the convergence rate as a function of ϵ of $\bar{c}(\alpha)$ to the exact $\bar{c}(\alpha)$. We used $\alpha = (\cos(3\pi/4), \sin(3\pi/4))$ for the circle pattern §5.1. Similar results were observed for the other patterns.

In conclusion, the best accuracy is achieved when the two values of ϵ were chosen to be the two largest cell sizes such that the grid directions $\{q_i\}$ all lie on corners of periodic cells, and Richardson's extrapolation is applied. When we used 24 directions, $\{q_i\}$, the best choice was $\epsilon = 1/3$ and $1/6$.

5.5. **Front propagation in random media.** We now consider a random media. Consider a random checkerboard structure, where in each cell the
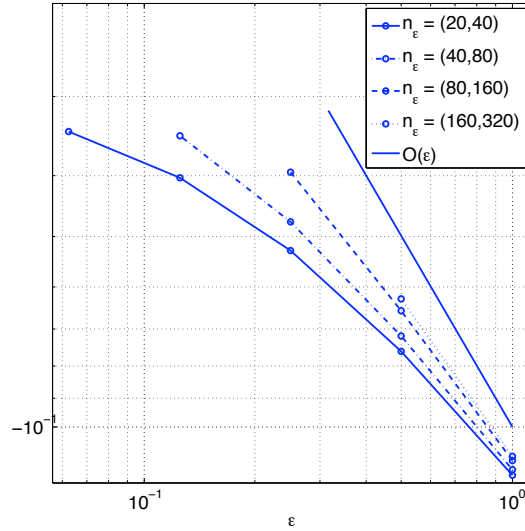
Figure 13: Convergence rate in ϵ for various cell resolutions n_ϵ.   `circleepsiloninterp`

`extrapetable`

pattern	exact $f_0(\alpha)$	error for $h = \epsilon/25, \epsilon/50$ $\epsilon = 1/24$	error for $h = \epsilon/25, \epsilon/50$ $\epsilon = 1/12, 1/24$	error for $h = \epsilon/100, \epsilon/200$ $\epsilon = 1/3, 1/6$
Checkerboard	1	-2.46E-02	-1.64E-02	-3.25E-03
Squares	$1/\sqrt{2}$	9.70E-04	9.65E-04	6.54E-05
Circles	0.90031	-5.10E-02	-4.74E-02	-1.70E-02
Stripes	0.70051	-2.58E-03	-1.53E-02	-1.60E-06

Table 1: Errors in $\bar{c}(\alpha)$ using extrapolation in: h only; h and ϵ (ϵ small); h and ϵ (ϵ large).

speed

$$c(x) = \begin{cases} 1 & \text{with probability } 0.5 \\ c_0 > 1 & \text{with probability } 0.5 \end{cases}$$

In this section, computations were performed using higher resolution, but plots use coarser computations for visualization purposes. Sample optimal paths are shown in Figure 4 for two different values of c_0, and with $\epsilon = 1/40$. Experimentally, the homogenized speed $\bar{c}(\alpha)$ is anisotropic; the vectogram is a circle. Compuations were performed averaging over 20 trials, and sampling 24 sampled directions. Any particular instance gave an approximate circle, but if $\bar{c}(\alpha)$ is averaged for each direction α over several computations, the result is circular.

The mean and variance of $\bar{c}$ were computed, as a function of c_0. In each case, the variance was less than 10^{-3}. Figure 14 shows the averaged $\bar{c}(\alpha)$ for $\epsilon = 0.01$ on a 2000^2 grid (but plotted on an 80^2 grid) and the ENO interpolated vectogram with 24 sampled directions, averaged over 20 trials. The dependance of $\bar{c}$ on the value c_0 is also plotted, It was more informative to plot $\bar{b} = 1/\bar{c}$ as a function of $1/c_0$., see Figure 14.

Remark (Average cost in the random case). An upper bound for the homogenized cost is the average of the costs in each cell. This is achieved by paths moving in a straight line in the direction α. But since optimal paths can wander to lower cost cells, the actual computed cost is lower. Better upper bounds can be achieved by estimating the probability that a neighboring cell is low cost. We are not aware of any known formulas for the homogenized speed in this case.
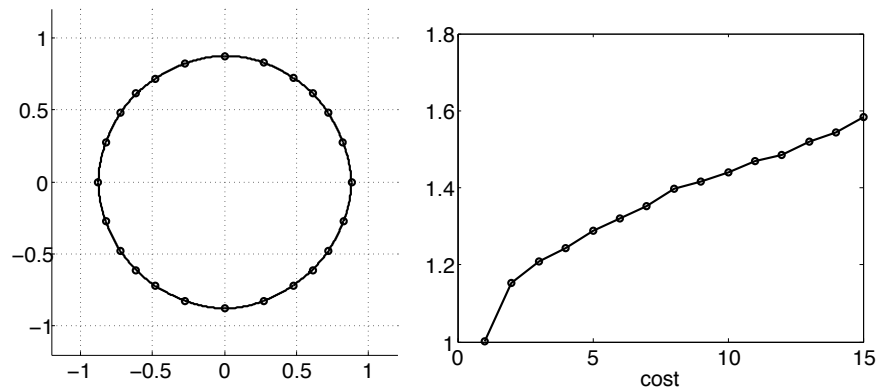

Figure 14: Illustration of the homogenized speed/cost in the random case. `randomMV` Left: computed vectogram, averaged over several trials, for $c = 1, 1/2$ with probability $1/2$. Right: computed homogenized cost $\bar{b}$ as a function of the random cost $b = 1$, or $b = b_0 = 1/c_0$ with probability $1/2$.

`randomConeCircle`

References

`homogChecker` 1. M. Amar, G. Crasta, and A. Malusa, *On the finsler metrics obtained as limit of chessboard structures*, available as `http://cvgmt.sns.it/papers/amacramal08/`, 2008.

`HomogFinsler` 2. M. Amar and E. Vitali, *Homogenization of periodic Finsler metrics*, J. Convex Anal. **5** (1998), no. 1, 171–186. MR MR1649453 (99k:49026)

`FinslerBook` 3. D. Bao, S.-S. Chern, and Z. Shen, *An introduction to Riemann-Finsler geometry*, Graduate Texts in Mathematics, vol. 200, Springer-Verlag, New York, 2000. MR MR1747675 (2001g:53130)

`BardiNotes` 4. Martino Bardi, *Some applications of viscosity solutions to optimal control and differential games*, Viscosity solutions and applications (Montecatini Terme, 1995), Lecture Notes in Math., vol. 1660, Springer, Berlin, 1997, pp. 44–97. MR MR1462700 (98f:49029)

`bornemann`   5. Folkmar Bornemann, *Fast eikonal solver in 2d*, available as `http://www-m3.ma.tum.de/twiki/bin/view/Software/FMWebHome`.

`BoydBook`   6. Stephen Boyd and Lieven Vandenberghe, *Convex optimization*, Cambridge University Press, Cambridge, 2004. MR MR2061575 (2005d:90002)

`BraidesBook`   7. Andrea Braides and Anneliese Defranceschi, *Homogenization of multiple integrals*, Oxford Lecture Series in Mathematics and its Applications, vol. 12, The Clarendon Press Oxford University Press, New York, 1998. MR MR1684713 (2000g:49014)

`IshiiCD`   8. I. Capuzzo-Dolcetta and H. Ishii, *On the rate of convergence in homogenization of Hamilton-Jacobi equations*, Indiana Univ. Math. J. **50** (2001), no. 3, 1113–1129. MR MR1871349 (2002j:35027)

`FinslerNotices`   9. Shiing-Shen Chern, *Finsler geometry is just Riemannian geometry without the quadratic restriction*, Notices Amer. Math. Soc. **43** (1996), no. 9, 959–963. MR MR1400859 (97e:53129)

`concordel`   10. Marie C. Concordel, *Periodic homogenisation of Hamilton-Jacobi equations. II. Eikonal equations*, Proc. Roy. Soc. Edinburgh Sect. A **127** (1997), no. 4, 665–689. MR MR1465414 (2000c:35012)

`BhattacharyaFronts` 11. Bogdan Craciun and Kaushik Bhattacharya, *Homogenization of a Hamilton-Jacobi equation associated with the geometric motion of an interface*, Proc. Roy. Soc. Edinburgh Sect. A **133** (2003), no. 4, 773–805. MR MR2006202 (2004m:35017)

`VSCL`   12. Michael G. Crandall and Pierre-Louis Lions, *Viscosity solutions of Hamilton-Jacobi equations*, Trans. Amer. Math. Soc. **277** (1983), no. 1, 1–42. MR MR690039 (85g:35029)

`ougandisEngquistReview` 13. B. Engquist and P. E. Souganidis, *Asymptotic and numerical homogenization*, Acta Numer. **17** (2008), 147–190. MR MR2436011

`EvansBook`   14. Lawrence C. Evans, *Partial differential equations*, Graduate Studies in Mathematics, vol. 19, American Mathematical Society, Providence, RI, 1998. MR MR1625845 (99e:35001)

`ObermanGomes`   15. Diogo A. Gomes and Adam M. Oberman, *Computing the effective Hamiltonian using a variational approach*, SIAM J. Control Optim. **43** (2004), no. 3, 792–812 (electronic). MR MR2114376 (2006a:49049)

`HolmesBook`   16. Mark H. Holmes, *Introduction to perturbation methods*, Texts in Applied Mathematics, vol. 20, Springer-Verlag, New York, 1995. MR MR1351250 (96j:34095)

`IsaacsBook`   17. Rufus Isaacs, *Differential games. A mathematical theory with applications to warfare and pursuit, control and optimization*, John Wiley & Sons Inc., New York, 1965. MR MR0210469 (35 #1362)

`BourliouxFronts` 18. Boualem Khouider and Anne Bourlioux, *Computing the effective Hamiltonian in the Majda-Souganidis model of turbulent premixed flames*, SIAM J. Numer. Anal. **40** (2002), no. 4, 1330–1353 (electronic). MR MR1951897 (2003m:76099)

`LionsPapVar`   19. Pierre-Louis Lions, George Papanicolaou, and S.R.S. Varadhan, *Homogenization of Hamilton-Jacobi equations*.

`StuartBook`   20. Grigorios A. Pavliotis and Andrew M. Stuart, *Multiscale methods*, Texts in Applied Mathematics, vol. 53, Springer, New York, 2008, Averaging and homogenization. MR MR2382139

`QianHomog`   21. J Qian, *Two approximations for effective hamiltonians arising from homogenization of Hamilton–Jacobi equations*, `http://www.math.ucla.edu/applied/cam/`, 2003.

`RorroHomog`   22. M. Rorro, *An approximation scheme for the effective Hamiltonian and applications*, Appl. Numer. Math. **56** (2006), no. 9, 1238–1254. MR MR2244974 (2007e:65093)

`SethianVladOUM`   23. James A. Sethian and Alexander Vladimirsky, *Ordered upwind methods for static Hamilton-Jacobi equations: theory and algorithms*, SIAM J. Numer. Anal. **41** (2003), no. 1, 325–363 (electronic). MR MR1974505 (2004f:65161)

`SoconolfiMetricHJ` 24. Antonio Siconolfi, *Metric character of Hamilton-Jacobi equations*, Trans. Amer. Math. Soc. **355** (2003), no. 5, 1987–2009 (electronic). MR MR1953535 (2005k:35043)

VladThesis 25. Alexander Vladimirsky, *Fast methods for static Hamilton-Jacobi Partial Differential Equations*, Ph.D. thesis, University of California, Berkeley, 2001.

DEPARTMENT OF MATHEMATICS, SIMON FRASER UNIVERSITY
E-mail address: `aoberman@sfu.ca`

DEPARTMENT OF MATHEMATICS, UNIVERSITY OF CALIFORNIA, LOS ANGELES
E-mail address: `rrtakei@ucla.edu`

DEPARTMENT OF MATHEMATICS, CORNELL UNIVERSITY
E-mail address: `vlad@math.cornell.edu`